JOURNAL OF MATERIALS SCIENCE 31 (1997) 3733–3738

Dislocations studies in β-silicon nitride

X. MILHET, H. GAREM, J. L. DEMENET, J. RABIER
Laboratoire de Métallurgie Physique, URA 131 CNRS, Université de Poitiers, UFR Sciences-SP2MI, Bd. 3 Téléport 2 BP 179, 86960 Futuroscope cedex, France

T. ROUXEL
Laboratoire des Matériaux Céramiques et Traitements de Surface, ENSCI, URA 320 CNRS, 47 Av. A. Thomas, 87065 Limoges, France

Some preliminary results of dislocation analysis and associated glide systems in as-grown as well as in superplastically deformed β silicon nitride are presented. Transmission electron microscopy observations using the weak-beam technique, are reported. $[0\,0\,0\,1]\,\{1\,0\,\bar{1}\,0\}$ and $1/3\langle 1\,\bar{2}\,1\,0\rangle\,\{1\,0\,\bar{1}\,1\}$ glide systems have been characterized. In the basal plane, a superposition of two hexagonal networks built with screw dipoles has been observed. Both a sequence extended node–constricted node and partial dislocations have been identified in these networks which clearly evinces dislocation dissociation in β-silicon nitride following the reaction $1/3\langle 2\,\bar{1}\,\bar{1}\,0\rangle \rightarrow 1/3\langle 1\,0\,\bar{1}\,0\rangle + 1/3\langle 1\,\bar{1}\,0\,0\rangle$.

1. Introduction

Silicon nitride, Si_3N_4, is a covalently bonded thermomechanical ceramic. The high-temperature mechanical properties of this compound are of great interest for industrial applications. However, its brittleness, as well as the lack of cheap and reliable shaping techniques, still prevent use of this material on a large scale. This has motivated research for new processing and shaping routes and recently, a superplastic Si_3N_4 was successfully synthesized [1–4]. Such deformation behaviour results mainly from grain-boundary sliding; however, it seems important, for a complete understanding of silicon nitride deformation mechanisms, to perform detailed analysis of dislocation configurations as well as slip systems characterization. This paper presents some preliminary results obtained by transmission electron microscopy (TEM) of dislocation configurations and slip systems in β silicon nitride.

2. Structure of silicon nitride

Silicon nitride exists with two different crystallographic modifications: the α phase, the metastable one, crystallizes above 1300 °C, and the β phase, the stable one, above 1700 °C. The reaction $\alpha \rightarrow \beta$ has been found to occur, but not the reverse one [5].

α- and β-Si_3N_4 have a hexagonal structure with, respectively, P_{31c} and $P_{6/3m}$ symmetry group [5–7]. The structure of the α-phase can be described by the piling up of four planes A, B, C, D, spaced out by $c_\alpha/4$, each of them containing a planar arrangement of three silicon and four nitrogen atoms (Fig. 1). The lattice parameters are $a_\alpha = 0.7753$ nm, $c_\alpha = 0.5618$ nm. The structure of the β-phase is a piling up of two planes A, B, spaced out by $c_\beta/2$, with an atomic arrangement similar to the α-phase (Fig. 2). The lattice parameters are $a_\beta = 0.7606$ nm, $c_\beta = 0.2909$ nm. Owing to the similarity between the two structures, c_α could be expected to be twice as large as c_β. However, the volume of the interstitial sites is smaller in the α structure; this results from atomic rearrangements and explains the variance of ratio c_β/c_α from 1/2 [6].

3. Previous dislocation observations

Some papers have been already published on dislocation observations in α- and β-Si_3N_4. Most of the studies have been performed on non-deformed silicon nitride.

3.1. Dislocations in α-Si_3N_4

In the α structure, $c[0\,0\,0\,1]$ is the most probable Burgers vector: dislocations with such a Burgers vector have been observed by several authors [8, 9]. Moreover, evidence of dislocation dissociation following the reaction $[0\,0\,0\,1] \rightarrow 1/2[0\,0\,0\,1] + 1/2[0\,0\,0\,1]$ has been provided [9]. In addition, dislocations with $a/3\langle 1\,1\,\bar{2}\,0\rangle$ Burgers vector have been observed several times by TEM in as-sintered materials [8–10] and also after deformation [11]. Associated with this Burgers vector, $\{1\,\bar{1}\,0\,1\}$ was found to be the primary glide plane [11]. $1/3\langle 1\,1\,\bar{2}\,3\rangle$ has also been reported as a possible Burgers vector [8, 9, 12], with the $\{\bar{1}\,\bar{1}\,2\,1\}$ habit plane [12]. Recently, Zhou and Mitchell [9] have characterized $\{1\,0\,\bar{1}\,0\}$ planes to be the glide planes of these three types of dislocations in chemical vapour deposited (CVD) material. Dislocations with $1/9\langle 1\,1\,\bar{2}\,3\rangle$ Burgers vector have been also observed by Suematsu *et al.* [13].

3.2. Dislocations in β-Si_3N_4

A theoretical analysis on Burgers vectors and different glide planes in β-silicon nitide has been performed by

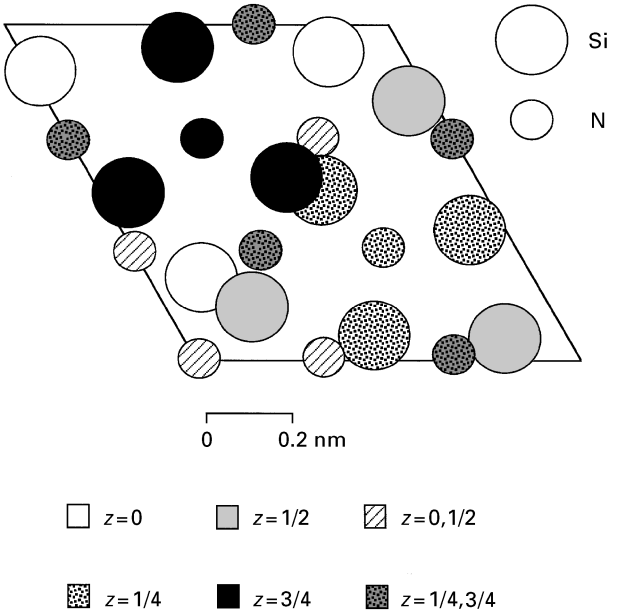

Figure 1 Basal projection of the α-silicon nitride unit cell.

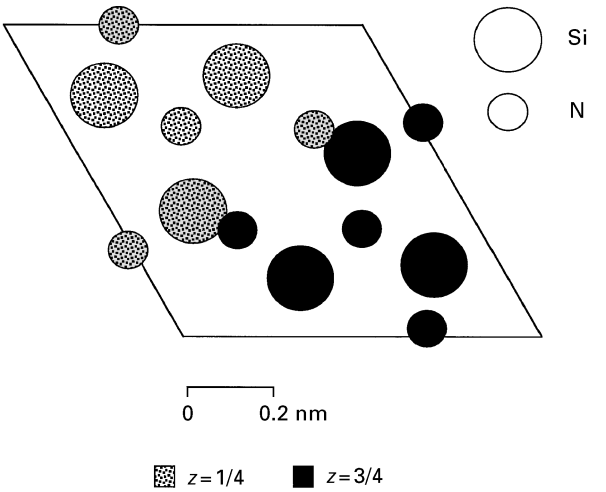

Figure 2 Basal projection of the β-silicon nitride unit cell.

Evans and Sharp [14]. They found that $c[0001]$, the shortest vector of the Bravais lattice, is the most probable Burgers vector for dislocations. This has been confirmed by several observations [14–17]. $\{10\bar{1}0\}$, $\{11\bar{2}0\}$, $\{12\bar{3}0\}$ have been proposed to be the three major glide planes [14]. The Burgers vector $a/3[11\bar{2}0]$, larger than the $c[0001]$ one, has also been observed in a β-Si_3N_4 by Hwang and Chen [16] and Lee and Hilmas [17]; however, this vector, predicted as a possible Burgers vector [14], has not often been observed. Evans and Sharp [14] also expected a possible dislocation reaction $c[0001] + a/3[11\bar{2}0] \rightarrow 1/3[11\bar{2}3]$. Even though this latest vector has been already observed [17–19], there is no evidence of the existence of partials which could have stabilized dislocations with such a large Burgers vector.

4. Experimental procedure

Structural defects in two different types of silicon nitride were analysed in this study. Material A is a pressureless sintered silicon nitride (SSN) with 3 wt% Al_2O_3 and 8 wt% Y_2O_3 as additives. The microstructure of this material is built mainly of β-Si_3N_4 grains, with a small amount of secondary intergranular glassy phase. Material B is obtained by hot pressing of Si_3N_4 powder (UBE-SNE10) containing 3 wt% Al_2O_3 and 6 wt% Y_2O_3 in a graphite die under a nitrogen flow. This results in a fine-grained material with a composition (determined by X-ray analysis) close to 70% α-phase and 30% β-phase. A tensile test performed on a sample of material B at 1595 °C using a strain rate of $2.5 \times 10^{-5}\,s^{-1}$ led to 85% deformation, demonstrating the suitability of this material to plastic forming techniques [4]. This high-temperature tensile test led to a final α/β ratio close to 23/77 [4].

For TEM studies, slices of about 200 μm were cut from these samples with a wire saw. After mechanical grinding and dimpling, the final thinning was achieved by argon ion milling at 5 kV in a Gatan duo mill. To prevent charging in the microscope, specimens were coated with an amorphous carbon layer. TEM observations were performed with a Jeol 200 CX microscope, operating at an accelerating voltage of 200 kV, with a double tilt specimen holder.

5. Results and discussion

Defects were observed mainly in β-Si_3N_4, which appeared to be the plastic phase as compared to the dislocation density found inside the grains. Because the investigated materials were processed at high temperature, the habit planes of dislocations were, when possible, determined by tilting the specimens in order to check whether the observed configurations result from glide or climb movements. This allowed unambiguous conclusions to be drawn about the dislocation glide planes.

5.1. Material A

TEM reveals elongated β-grains, as characterized by diffraction pattern analysis, containing complex dislocation arrangements. Fig. 3a and b show a typical dislocation microstructure which is built of several dislocation families which are referenced E, F, G and H. E dislocations are the main dislocation family of this microstructure. They appear as long straight segments which bow out of this orientation on the left part of the figure and can interact in some places with H dislocations. E dislocations are out of contrast for the $hki0$ reflections so that their Burgers vector is $c[0001]$. The orientation of their long straight segment is along $c[0001]$ so that they have a screw orientation on most of their length. When these dislocations bow out of this screw orientation, their line orientation, determined by tilting experiments, belongs to $\{10\bar{1}0\}$. This determination is consistent with a glide system $[0001]\ \{10\bar{1}0\}$ and a strong Peierls potential along the screw direction.

The Burgers vector of H dislocations interacting with E dislocations has been determined to be $1/3[1\bar{2}10]$. A trace analysis of the short H dislocation

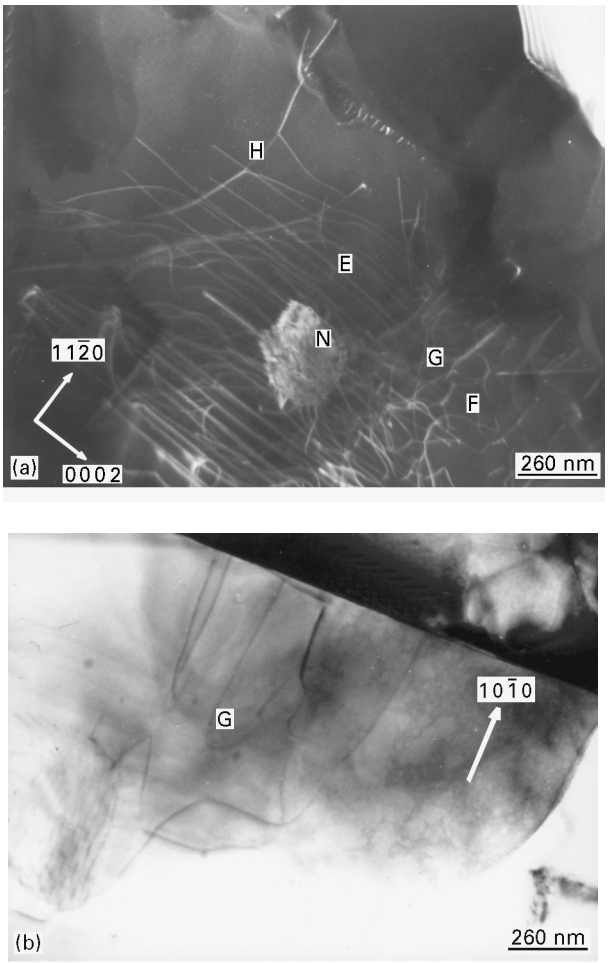

Figure 3 Pressureless sintered silicon nitride (material A). Burgers vectors of the dislocations characterized in the grain: E, $\boldsymbol{b} = [0001]$; F, $\boldsymbol{b} = 1/3[1\bar{2}13]$; G, $\boldsymbol{b} = 1/3[\bar{2}11x]$; H, $\boldsymbol{b} = 1/3[1\bar{2}10]$. (a) Weak-beam dark-field, $\boldsymbol{g} = [0002]$, $s_g = 7.1 \times 10^{-2}$ nm^{-1}. (b) Bright-field, $\boldsymbol{g} = [10\bar{1}0]$.

segments which have not interacted with E dislocations, leads to an average direction at 60° from $[1\bar{2}10]$ and an habit plane $\{10\bar{1}1\}$. This type of glide system $1/3[1\bar{2}10]$ $\{10\bar{1}1\}$ has also been previously observed by Suematsu *et al.* [11] in α-Si_3N_4. Fig. 4

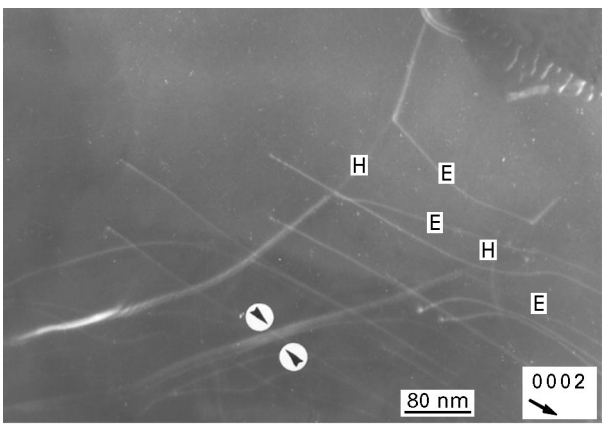

Figure 4 Enlargement of the left side of the grain studied in material A: reaction between E and H dislocations, following the reaction $[0001] + 1/3\langle 1\bar{2}10\rangle \rightarrow 1/3\langle 1\bar{2}13\rangle$. Dislocations and Burgers vectors involved in the reaction: H1, H2, $\boldsymbol{b} = a/3\langle 1\bar{2}10\rangle$; E1, E2, E3, $\boldsymbol{b} = c[0001]$; α1, β1, β2, $\boldsymbol{b} = 1/3\langle 1\bar{2}13\rangle$; α2, $\boldsymbol{b} = 1/3\langle \bar{1}2\bar{1}3\rangle$. Weak-beam dark-field, $\boldsymbol{g} = [0002]$, $s_g = 7.1 \times 10^{-2}$ nm^{-1}.

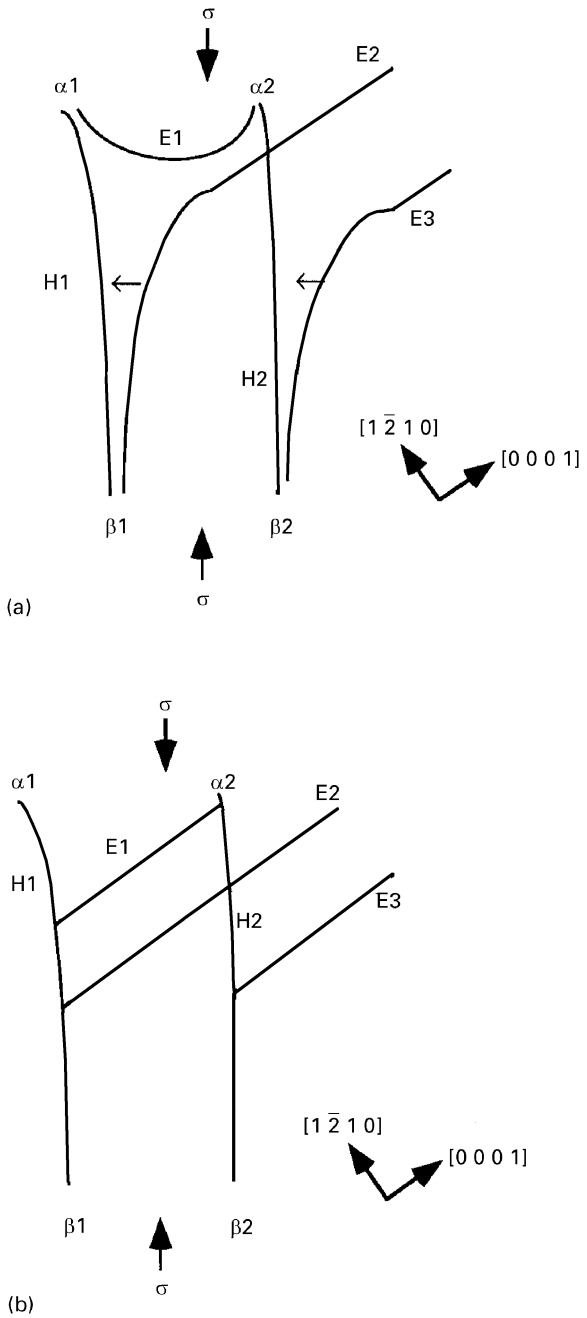

Figure 5 Proposed mechanism for the creation of the arrangement shown in Fig. 4: dislocations with $c[0001]$ Burgers vector, E1, E2 and E3, glide under the action of local stress (a), leading to reaction with dislocations with $a/3\langle 1\bar{2}10\rangle$ Burgers vector H1 and H2 at points α1, α2, β1, β2 (b).

focuses on the E, H interactions and Fig. 5a and b address the dislocation reactions. Several E dislocations, E1, E2 and E3, interact with two H dislocations, H1 and H2, following the reactions

$$E1 + H1 \rightarrow \alpha 1 \quad (1)$$

$$-E1 + H2 \rightarrow \alpha 2 \quad (2)$$

$$E2 + H1 \rightarrow \beta 1 \quad (3)$$

$$E3 + H1 \rightarrow \beta 2 \quad (4)$$

The dislocation junctions α1, β1, β2 have the same Burgers vector $1/3[1\bar{2}13]$. Indeed, these dislocations are out of contrast with $10\bar{1}0$ and in contrast with 0002, while α2 has a $1/3[\bar{1}2\bar{1}3]$ Burgers vector.

These reactions can be written for α1, β1, β2

$$c[0001] + a/3[1\bar{2}10] \rightarrow 1/3[1\bar{2}13] \quad (5)$$

and for α2

$$c[0001] - a/3[1\bar{2}10] \rightarrow 1/3[\bar{1}2\bar{1}3] \quad (6)$$

These reactions involve no gain in elastic energy as far as isotropic elasticity is concerned, and can be favoured by local stress effects or elastic anisotropy. The occurrence of the two different reactions is in agreement with local stress effects which probably result from the process (Fig. 5a). Other E dislocations crossing the resultant dislocations junctions β1, β2 do not interact with those dislocations, because they are probably far enough from the plane of the arrangement. However, some of them pile up along β2 building multipoles (see arrows in Fig. 4). Besides these main features of the dislocation arrangements, several other dislocations are evinced (see Fig. 3).

In the network, N, the density of dislocations is too important for an unambiguous characterization of the Burgers vector and the direction of each type of dislocations lines. Many of the dislocations in this network are out of contrast when using the $10\bar{1}0$ type reflections. This is consistent with a basal plane component for their Burgers vector.

G dislocations located near network N are out of contrast for the reflection $01\bar{1}0$ but in contrast for all the other $hki0$ reflections (Fig. 3). Their Burgers vector could be of the type $1/3[\bar{2}11x]$. Because of the large density of dislocations with $c[0001]$ Burgers vector imaged with the 0002 reflection, visibility or extinction of G dislocations is difficult to check: an unambiguous determination of the x component has not been achieved.

F dislocations are in contrast with the two $1\bar{1}01$ and 0002 reflections and are out of contrast with $10\bar{1}0$. Their probable Burgers vector is $1/3[1\bar{2}13]$ which has been previously observed [17–19], although the associated strain energy is expected to be very large. They probably appear as dislocation junctions. A trace analysis of the dislocation line shows that the average direction is near $[1\bar{1}01]$, but the habit plane of these dislocations has not been determined.

Characteristics of all the dislocations found in Fig. 3 are summarized in Table I.

5.2. Material B

This material has a smaller grain size than material A; the β structure of the few larger grains has been unambiguously determined by diffraction patterns. Many dislocations are evinced in those grains; the smaller the grains, the lower is the dislocation density. Among the dislocation configurations, the configuration shown in Fig. 6 was characterized. This configuration is built with several dislocation families arranged mainly as an hexagonal network. This network has been found to lie in the basal plane $\{0001\}$ (Fig. 6).

Dislocations are in contrast for only two of the three $10\bar{1}0$ reflections. Their Burgers vector is then $\boldsymbol{b} = 1/3\langle 11\bar{2}x\rangle$. Most of the dislocations are located at 60° from each other. The plane of the network and the line direction of the dislocations, parallel to the three $\langle 1\bar{2}10\rangle$ directions, are consistent with dislocations with $a/3\langle 1\bar{2}10\rangle$ Burgers vector lying along the screw direction. The network results from dislocation reactions of the type

$$a/3[11\bar{2}0] + a/3[\bar{2}110] \rightarrow a/3[\bar{1}2\bar{1}0] \quad (7)$$

Reflections $\boldsymbol{g} = 20\bar{2}0$ $1\bar{2}10$, and $12\bar{3}0$, evince a dissociation of dislocations through the observation of a sequence of extended and constricted nodes (Figs 7 and 8). This observation is consistent with the dissociation reaction $1/3\langle 2\bar{1}\bar{1}0\rangle \rightarrow 1/3\langle 10\bar{1}0\rangle + 1/3\langle 1\bar{1}00\rangle$ and the existence of two stacking fault energies with very different values (in analogy with fcc and hcp metals). These partial dislocations at the extended nodes can be clearly identified using

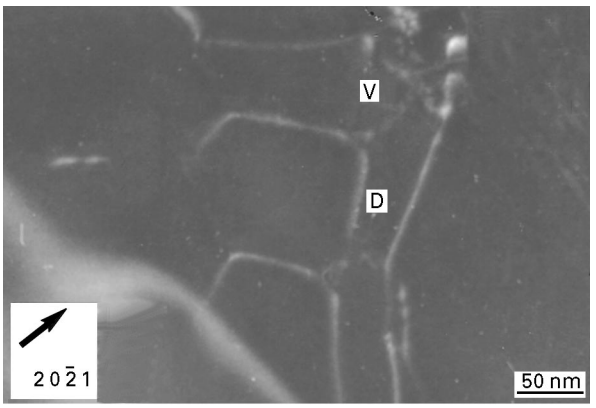

Figure 6 Screw dislocation network viewed with $20\bar{2}1$ reflection in material B. Most of the dislocations have a Burgers vector $a/3\langle 1\bar{2}10\rangle$ and react leading to a sequence of constricted and extended nodes. A reaction between a dislocation, with a Burgers vector $1/3\langle 1\bar{2}10\rangle$, with V dislocation, with $c[0001]$ Burgers vector, gives the dislocation D with a Burgers vector $1/3\langle 1\bar{2}13\rangle$. Weak-beam dark-field, $\boldsymbol{g} = [20\bar{2}1]$, $s_g = 7.9 \times 10^{-2}\ \mathrm{nm}^{-1}$.

TABLE I Characteristics of dislocations of Figs 3 and 4

Dislocations	$\boldsymbol{b}$	$\boldsymbol{l}$	$\boldsymbol{b} \wedge \boldsymbol{l}$	Habit plane[a]
E	[0001]	[0001]; $[1\bar{2}11]$	$\{10\bar{1}0\}$	$\{10\bar{1}0\}$
F	$1/3[1\bar{2}13]$	$[1\bar{1}01]$	$\{01\bar{1}1\}$	?
G	$1/3[\bar{2}11x]$	?	?	?
H	$1/3[1\bar{2}10]$	?	?	$\{10\bar{1}1\}$
α1, β1, β2	$1/3[1\bar{2}13]$	?	?	$\{10\bar{1}1\}$
α2	$1/3[\bar{1}2\bar{1}3]$	?	?	$\{10\bar{1}1\}$

[a] Habit plane determined by tilting experiments.

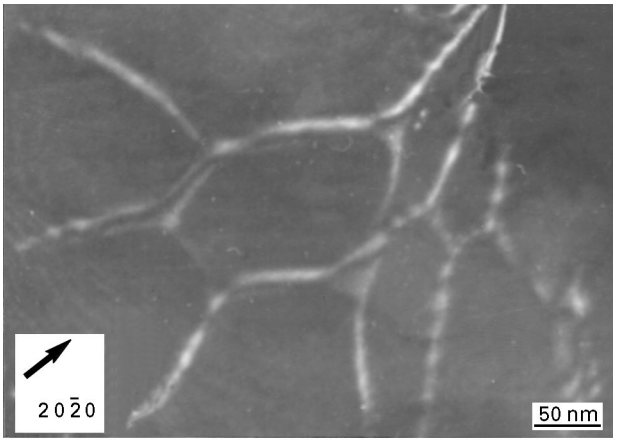

Figure 7 Evidence of two superposed networks in material B. Weak-beam dark-field, $\boldsymbol{g} = [20\bar{2}0]$, $s_g = 5.4 \times 10^{-2}\,\mathrm{nm}^{-1}$.

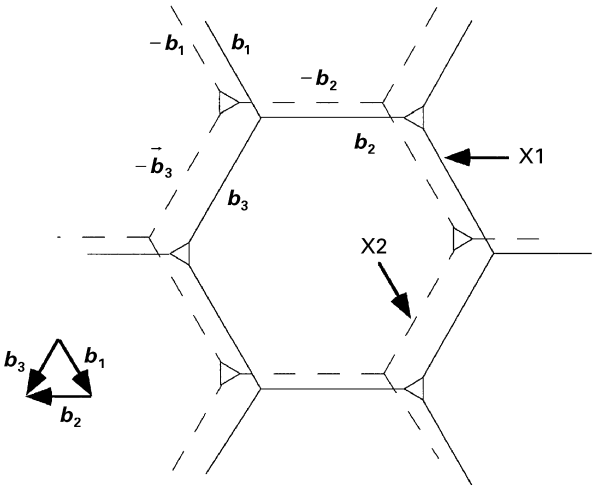

Figure 8 Arrangement of the two superimposed networks X1 and X2 built with screw dislocations. Dissociation at nodes yields to the superposition of extended and constricted nodes (see Fig. 9). $\boldsymbol{b}_1 = a/3[1\bar{2}10]$; $\boldsymbol{b}_2 = a/3[\bar{2}110]$; $\boldsymbol{b}_3 = a/3[\bar{1}\bar{1}20]$.

reflections $10\bar{1}0$ and $1\bar{2}10$. However, for some diffracting conditions, the same node sometimes appears extended and sometimes constricted. Indeed, imaging with $20\bar{2}0$ and $30\bar{3}0$ diffracting vectors, which have lower extinction distances than $10\bar{1}0$, shows that this network is built with two parallel networks of screw dislocations (Figs 7 and 8). $\pm\boldsymbol{g}$ imaging conditions provide the evidence that screw dislocation dipoles are involved in the network formations. Such a superposition of hexagonal dislocation networks has already been observed in zinc single crystals by G'Sell and Champier [20] and Tyapunina *et al.* [21]. Because the two superposed hexagonal networks have dislocations with opposite Burgers vectors, the superposition of an extended node of a network over a constricted node in the other network can be explained. Indeed, an extended node occurs for a specific composition rule, i.e. $\mathrm{AB} + \mathrm{BC} - \mathrm{AC} = 0$ of the three perfect dislocations (see, for example, Amelincks [22]), that is at α and α' (Fig. 9), whereas the neighbouring node has a different composition rule $\mathrm{AC} - \mathrm{BC} - \mathrm{AB} = 0$ consistent with a constricted node (β and β' in Fig. 9). These two composition rules are exchanged when the Burgers

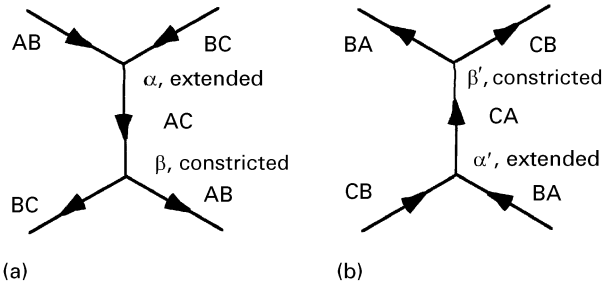

Figure 9 Extended–constricted node formation rule: at α, $\mathbf{AB} + \mathbf{BC} - \mathbf{AC} = \mathbf{0}$; at β, $\mathbf{AC} - \mathbf{BC} - \mathbf{AB} = \mathbf{0}$. (a) Dislocation network X1, (b) dislocation network X2.

vectors of the interacting dislocations are opposite, so that the extended node occurs at the place of a constricted one in the two different networks.

Another dislocation, V, which appears in weak contrast on Fig. 6 has been clearly identified with several different diffracting conditions and is characterized by a $c[0001]$ as a Burgers vector. Dislocation V interacts with dislocations of the hexagonal network X1 (cf Fig. 8) and leads to a dislocation junction with $1/3[1\bar{2}13]$ Burgers vector following the reaction

$$c[0001] + a/3[1\bar{2}10] \rightarrow 1/3[1\bar{2}13] \qquad (8)$$

The junction dislocation, included in the previous hexagonal network, does not have a screw character. This reaction seems to have occurred after the network formation.

The formation of such an hexagonal network built with dislocation dipoles is under investigation. It can result from plasticity events occurring during superplastic deformation or from small misorientation between β subgrains or a β–β' interface, as previously observed by Hwang and Chen [16].

6. Conclusion

TEM studies were performed on deformed and non-deformed silicon nitride. Most of the dislocations are located in β grains, most of them having a Burgers vector $\boldsymbol{b} = c[0001]$ and a glide plane $\{10\bar{1}0\}$. Another type of dislocation with $\boldsymbol{b} = a/3\langle 1\bar{2}10\rangle$ has been found to lie in the $\{10\bar{1}1\}$ slip planes and stabilized as a network in basal planes. Dislocations with Burgers vector $1/3\langle 1\bar{2}13\rangle$ were also shown to result from a reaction between dislocations with $c[0001]$ and $a/3\langle 1\bar{2}10\rangle$ Burgers vector. A superposition of two hexagonal networks in the basal plane composed by screw dipoles is observed. In this configuration, dislocation dissociation into partials through a sequence of constricted–extended nodes was evinced. This provides the first evidence for a dislocation dissociation of the type: $1/3\langle 2\bar{1}\bar{1}0\rangle \rightarrow 1/3\langle 10\bar{1}0\rangle + 1/3\langle 1\bar{1}00\rangle$ in β-Si_3N_4. The mechanism for the dipole network formation is under investigation.

Acknowledgements

We thank Dr M. Bougoin, Céramiques et Composites (Bazet, FRANCE), for providing specimens of grade A,

and Dr F. Rossignol and Professor P. Goursat, LMCTS (Limoges, FRANCE), for the preparation of material B.

References

1. F. WAKAI, Y. KODAMA, S. SAKAGUCHI, N. MURAYAMA, K. IZAKI and K. NIIHARA, *Lett. Nature* **344** (1990) 321.
2. I. W. CHEN and L. A. XUE, *J. Am. Ceram. Soc.* **73** (1990) 2585.
3. T. ROUXEL, F. ROSSIGNOL, P. GOURSAT, J. L. BESSON, J. F. GOUJAUD and P. LESPADE, in "Plastic Deformation in Ceramics", edited by J. Routbort, R. C. Bradt and C. Brooks (Plenum Press, New York, London, 1995) p. 351.
4. F. ROSSIGNOL, T. ROUXEL, J. L. BESSON, P. GOURSAT and P. LESPADE, *J. Phys. III* **5** (2) (1995) 127.
5. R. GRÜN, *Acta Crystallogr.* **B 35** (1979) 2157.
6. R. MARCHAND, Y. LAURENT and J. LANG, *ibid.* **B 25** (1969) 2157.
7. R. W. G. WYCKOFF, "Crystal Structures", Vol. 2, 2nd Edn (Interscience, New York, 1969) p. 157.
8. S. L. HWANG and I. W. CHEN, *J. Am. Ceram. Soc.* **77** (1994) 1711.
9. D. S. ZHOU and T. E. MITCHELL, *ibid.* **78** (1995) 3133.
10. C. H. WANG, F. L. RILEY, F. C. CASTRO and I. ITURIZA, *ibid.* **76** (1993) 2136.
11. H. SUEMATSU, J. J. PETROVIC and T. E. MITCHELL, *Mater. Res. Soc. Symp. Proc.* **287** (1993) 449.
12. K. L. MORE, in "Proceedings of the 49th Annual Meeting of the Electron Microscopy Society of America", edited by G. W. Bailey (San Francisco Press, San Francisco, CA, 1991) p. 936.
13. H. SUEMATSU, J. J. PETROVIC and T. E. MITCHELL, in "Proceedings of the 50th Annual Meeting of the Electron Microscopy Society of America", edited by G. W. Bailey, J. Bentley and J. A. Small (San Francisco Press, San Francisco, CA, 1992) p. 342.
14. A. G. EVANS and J. V. SHARP, *J. Mater. Sci.* **6** (1971) 1292.
15. E. BUTLER, *Philos. Mag.* **24** (1971) 829.
16. S. L. HWANG and I. W. CHEN, *J. Am. Ceram. Soc.* **77** (1994) 1719.
17. W. E. LEE and G. E. HILMAS, *ibid.* **72** (1989) 1931.
18. P. MARQUIS and E. BUTLER, *J. Mater. Sci. Lett.* **12** (1977) 424.
19. A. G. EVANS and J. V. SHARP, in "Electron Microscopy and Structure of Materials", edited by G. Thomas, R. M. Fulrath and R. M. Fisher (California Press, Berkeley, CA, 1972) p. 1141.
20. C. G'SELL and G. CHAMPIER, *Philos. Mag.* **32** (1975) 283.
21. N. A. TYAPUNINA, T. N. PASHENKO and G. M. ZINENKOVA, *Phys. Status Solidi* (*a*) **31** (1975) 309.
22. S. AMELINCKS, in "Dislocations in solids", edited by F. R. N. Nabarro (North Holland, Amsterdam, 1979) p. 435.

Received 6 February
and accepted 2 July 1996